

*Original Research*

# Insight into Adsorption of Cesium Ion in Aqueous Solution Based on Inorganic Modified Bentonite

Ji Chen<sup>1,2</sup>, Yuru Chen<sup>1</sup>, Yu Zhou<sup>1</sup>, Xinyu Luo<sup>1</sup>, Qiang Tang<sup>1,2\*</sup>

<sup>1</sup>School of Rail Transportation, Soochow University, Xiangcheng District, Suzhou, 215131, China

<sup>2</sup>Graduate School of Global Environmental Studies, Kyoto University, Sakyo-ku, Kyoto, 606-8501, Japan

*Received: 4 November 2022*

*Accepted: 28 December 2022*

## Abstract

Bentonite, with excellent osmotic swelling performance and low hydraulic conductivity, represents as an ideal material for the final disposal of radioactive wastes. This paper investigates bentonite and three inorganic modified bentonites (Na-Bentonite, K-Bentonite and Mg-Bentonite) in adsorption of Cs<sup>+</sup>, one of the major hazardous metals in radioactive waste. The effects of solution pH value, sorbent dosage and initial concentration on the adsorption performance of Cs<sup>+</sup> were investigated, as well as the effects of temperature and reaction time on the adsorption capacity and removal rate of heavy metal Cs<sup>+</sup>. The internal structure and chemical composition of bentonite before and after adsorption were also discussed. The results indicate that the maximum adsorption rate is 95.30%, and the estimated best adsorption capacity is almost 28.2 mg/g. 1.1 g bentonite dosage and 1.0 mol/L solution concentration in alkaline environment is the most suitable conditions for cesium adsorption reaction, which can be witnessed in Na-Bentonite.

**Keywords:** cesium, modified bentonite, adsorption isotherms and kinetics, micro-scope mechanism

## Introduction

Nuclear technology represents a significant role in various fields, including energy, materials, medical treatment, etc. However, that leads to a large amount of radioactive industrial waste, which is hard to handle [1, 2]. In addition to industrial production, the discharge of radioactive pollutants may also be caused by force majeure disasters, such as the leakage of Fukushima nuclear power plant in 2011 caused by the tsunami [3, 4]. In the most circumstances, radionuclides are in a cationic state with water as the

medium. And among these fission nuclides, <sup>134</sup>Cs and <sup>137</sup>Cs are important radioactive heavy metal pollutant, which presents high radioactivity, high mobility, with a half-life of 30 years, and may migrate continuously in the environment [5]. Once absorbed by human, <sup>134</sup>Cs and <sup>137</sup>Cs release  $\beta$  and  $\gamma$  ray, which concentrated in human muscle and lead to cell carcinogenesis. It will further bring about long-term effects and genetic hazards such as leukemia, infertility or even fetal malformation [6, 7, 8]. Thus, improper handling will pose a threat to environmental security and even human health.

For the disposal of cesium, much researches on radionuclide treatment methods had been carried out. At present, radionuclide is mainly treated by inorganic, inorganic-polymer composites and

\*e-mail: tangqiang@suda.edu.cn

bio-adsorbents [9]. To be specific, the treatment methods can be summarized as chemical precipitation, solvent extraction, membrane separation, ion exchange and evaporation [10]. The use of a large number of salts in chemical precipitation method is likely to cause the anion or pH of precipitant in water exceeding the standard. Some extractants in solvent extraction are highly toxic, which makes the original toxic pollutant solution can't be treated essentially. In addition, the membrane separation method has high energy consumption and low recovery, while the membrane pollution remains a serious problem. Last but not least, the biological treatment requires strict treatment conditions, but may receive low treatment efficiency [11, 12]. In comparison, ion exchange/adsorption method has been widely used in the removal of radioactive elements and pollutant treatment in aqueous solution because of high efficiency, simplicity, high selectivity and strong adaptability [13, 14]. For cesium and other hazardous or radioactive waste metals, the main adsorption materials are clay minerals, natural/artificial zeolite, multivalent metal phosphate and composite ion exchange materials, metal ferrocyanide, titanium silicon compounds [10, 15, 16]. The clay minerals, with low permeability and good buffering performance, are often utilized in horizontal or vertical barriers in landfills. The bentonite is the most widely used clay mineral for underground disposal of radioactive wastes [17, 18]. Bentonite is a traditional clay mineral adsorption material and represents as an effective adsorption method to reduce radionuclides. High cation exchange capacity and large specific surface area exist in bentonite particles, providing sufficient surface adsorption pore sites. At the same time, the adsorption affinity of bentonite is also in high level. However, its tolerance in severe alkali environment is one of the disadvantages, and the negative charge on its surface is not feasible for effective ion exchange. To improve the adsorption performance, this paper used the inorganic method as acid activation for ion exchange modification. Actually, the cesium concentration is not constant, and it may diminish or increase with time passing. Therefore, in this paper we conducted a wider range of concentration to investigate the adsorption mechanism of cesium by modified bentonite.

In this paper, unmodified bentonite and three modified bentonite using ion-exchange method were utilized as adsorbents, while CsCl (Nonradioactive cesium) solution as solvent. The effects of reaction time and initial concentration were investigated, combing with adsorption kinetic and isothermal models to analyze the adsorption performance. Besides of this, we also researched on the effects of temperature, solution pH value and adsorbent dosage. For the internal structure and adsorption mechanism of bentonite before and after adsorption, scanning electron microscopy (SEM) and X-ray diffraction (XRD) tests were also conducted.

## Experimental

### Materials and Methods

#### *Preparation of Solutions and Sorbents*

The contaminated radionuclide researched in this paper is non-radioactive cesium chloride (CsCl), because of the similar properties with radioactive cesium [19, 20]. The selected sorbent is bentonite, which is purchased in Suzhou, China. The modified bentonite with different properties had been used and compared via modification process. The modified bentonite is modified by sodium chloride (NaCl), potassium chloride (KCl) and magnesium chloride (MgCl<sub>2</sub>) solution separately through ion exchange, and they are numbered as Bentonite, Na-Bentonite, K-Bentonite and Mg-Bentonite. All the reagents or chemicals used in the tests are analytical grade. Sodium hydroxide (NaOH) and hydrochloric acid (HCl) solution are used to investigate the effect of pH and acid-base conditions on the adsorption reaction. All test solutions were prepared with double-distilled water.

#### *Experiments*

##### Effect of Initial Concentration

1.0 g of bentonite was added into 50 ml of Cs<sup>+</sup> solution with ion concentrations of 0.1 mmol/L, 0.3 mmol/L, 0.5 mmol/L, 0.8 mmol/L and 1.0 mmol/L respectively, and the solid-liquid ratio is 1:50. When the pH value is 7, oscillate at the room temperature of 20°C at the speed of 150 R/min for 3 hours, equilibrium and static adsorption at 20°C for 8 hours, and then centrifuge at 4000 R/min for 10 minutes. The concentration of each ion in the supernatant was determined by atomic absorption spectrometry, and the adsorption capacity of each ion was calculated by subtraction method. Other than these, Initial Concentration of 3 mmol/L, 5 mmol/L and 8 mmol/L were also tested, but not included in this section. The aim was to investigate the influence of excess initial concentration, and these results are analyzed in isotherm model fitting. Cs<sup>+</sup> removal results were calculated based on the following equations [21, 22]. The equation of unit adsorption capacity at equilibrium is:

$$Q_e = \frac{(C_0 - C_e) \times V}{m} \quad (1)$$

The  $Q_e$  represents unit adsorption capacity at equilibrium.  $V$  is the volume of solution, and  $m$  is the weight of bentonite dosage.  $C_0$  and  $C_e$  are the concentration of Cs<sup>+</sup> before and after adsorption equilibrium (mmol/g) [23]. The removal rate of Cs<sup>+</sup> is shown as:

$$\eta = \frac{C_0 - C_t}{C_0} \times 100\% \quad (2)$$

In this formula,  $C_0$  and  $C_t$  represents the concentration before adsorption and the concentration at adsorption time of  $t$ .

#### Effect of Adsorption Reaction Time

1.0 g of bentonite was added into 50 ml of  $\text{Cs}^+$  solution with ion concentration of 0.1 mmol/L and solid-liquid ratio of 1:50. When the pH value is 7, oscillate at room temperature of 20°C at the speed of 150 R/min for 3 hours, balance and static adsorption at 20°C for 4, 6, 10 and 12 hours respectively, and then centrifuge at 4000 R/min for 10 minutes. Determine the concentration of each ion in the supernatant by atomic absorption spectrometry, the adsorption capacity of each ion was calculated by subtraction method.

#### Effect of Initial Concentration

1.0 g of bentonite was added into 50 ml of  $\text{Cs}^+$  solution with ion concentration of 0.1 mmol/L. when the pH value is 7, continue to add 0.1 g, 0.3g, 0.5 g, 1g and 1.5 g of bentonite or bentonite into the solution respectively. The solid-liquid ratio is 11:500, 13:500, 15:500, 20:500 and 25:500 respectively. Oscillate at the speed of 150 R/min at the room temperature of 20°C for 3 hours, and equilibrium static adsorption at 20°C for 8 hours, and then centrifuged at 4000 R/min for 10 min, the concentration of each ion in the supernatant was determined by atomic absorption spectrometry, and the adsorption capacity of each ion was calculated by subtraction method.

#### Effect of pH

1.0 g of bentonite was added into 50 ml of  $\text{Cs}^+$  solution with ion concentration of 0.1 mmol/L, adjust it to different pH values (3, 7, 11) with weak acid and weak base, with solid-liquid ratio of 1:50, oscillate at room temperature of 20°C at the speed of 150 R/min for 3 hours, equilibrium and static adsorption at 20°C for 8 hours, then centrifuge at 4000 R/min for 10 minutes, and determine the concentration of each ion in the supernatant by atomic absorption spectrometry, The adsorption capacity of each ion was calculated by subtraction method.

#### Effect of Temperature

1.0 g of bentonite was added into 50 ml of  $\text{Cs}^+$  solution with ion concentration of 1 mmol/L, solid-liquid ratio of 1:50, oscillate at room temperature of 20°C for 3 hours at pH value of 7, equilibrium and static adsorption at 40°C, 60°C and 80°C for 8 hours respectively, and then centrifuge at 4000 R/min for

10 minutes. Determine the concentration of each ion in the supernatant by atomic absorption spectrometry, The adsorption capacity of each ion was calculated by subtraction method. The impactors of pH and temperature were referring to previous research [24].

#### Adsorption Kinetics

Adsorption kinetics mainly presents an angle into the factors affecting the adsorption rate of some substances with large surface energy (such as bentonite), based on effect of temperature, reaction conditions, etc., to describe the dynamic process of adsorption. At present, the most widely used adsorption kinetic models include Pseudo first-order kinetic model, Pseudo second-order kinetic model and Intraparticle diffusion kinetic model [25].

The Pseudo-first-order kinetic model is shown as below:

$$Q_t = Q_e(1 - e^{-k_1 t}) \quad (3)$$

In equation (1),  $k_1$  is the adsorption rate constant,  $t$  is the reaction time,  $Q_e$  and  $Q_t$  are the adsorption amount at equilibrium and any time, respectively [26, 27].

Then, the formula (2) presented below is Pseudo-second-order kinetic model:

$$Q_t = \frac{k_2 Q_e^2 t}{1 + k_2 Q_e t} \quad (4)$$

$k_2$  is the adsorption rate constant, and other parameters possess the same meanings as in Pseudo-first-order kinetic model.

The third kinetic model used in this paper is Intraparticle diffusion kinetic model, which can monitor the step of adsorbent adsorption rate in an accurate way. The equation is written as:

$$Q_t = k_{int} t^{1/2} + C \quad (5)$$

In this equation,  $k_{int}$  is the correlation adsorption rate constants and  $C$  represents intercept on the axis [28, 29].

#### Adsorption Isotherms

Based on the results in effect of initial concentration, and intended for further research in the adsorption process. Langmuir isothermal model, Freundlich isothermal model and Redlich-Peterson (R-P) isothermal model were conducted for liner fitting and parameter analysis in this paper. The Langmuir isothermal model presents the surface adsorption performance of the material with physicochemical properties, and the equation is shown as below:

$$Q_e = \frac{Q_m K_L C_e}{1 + K_L C_e} \tag{6}$$

where  $Q_e$  is the equilibrium unit adsorption capacity,  $Q_m$  is the maximum adsorption capacity, and  $K_L$  is the equilibrium constant. The value of  $K_L$  is related to the type of adsorbent and adsorbate and temperature. The greater the  $K_L$  value, the better of the adsorption capacity [30, 31].

The equation of Freundlich isothermal model is written as below:

$$Q_e = K_F C_e^{1/n} \tag{7}$$

$K_F$  value is Freundlich adsorption characteristic constant, which generally decreases with the increase of temperature;  $1/n$  represents the adsorption efficiency (generally between 0 and 1), and the value represents the influence of mass concentration on the adsorption capacity. The smaller of  $1/n$ , the better the adsorption performance. When  $1/n > 2$ , the adsorption reaction is difficult to occur spontaneously [32].

In order to make up for the limitations of Langmuir isothermal model and Freundlich isothermal model,

this paper conducted Redlich-Peterson (R-P) isothermal model to study the test data, which is based on the improvement of Langmuir isothermal model [33]. The equation is described as below:

$$Q_e = \frac{K_{RP} C_e}{1 + a_{RP} C_e^\beta} \tag{8}$$

In this formula,  $K_{RP}$  and  $a_{RP}$  represents the characteristic constant of Redlich-Peterson (R-P) isothermal model.  $\beta$  is an index between 0 and 1. When  $\beta = 1$ , it can be simplified as Langmuir model, while it is an optimization and improvement based on this model. When  $\beta = 0$ , it can be simplified as Henry model.

### Sorbents Characterization

The solid-liquid ratio is 1:50 and the concentration of ionic solution is 2.0 mmol/L. after the reaction, the solid residue then packed for inspection. Through SEM and XRD tests, it is compared with the different indexes of modified bentonite to study the reaction micro-scope mechanism.

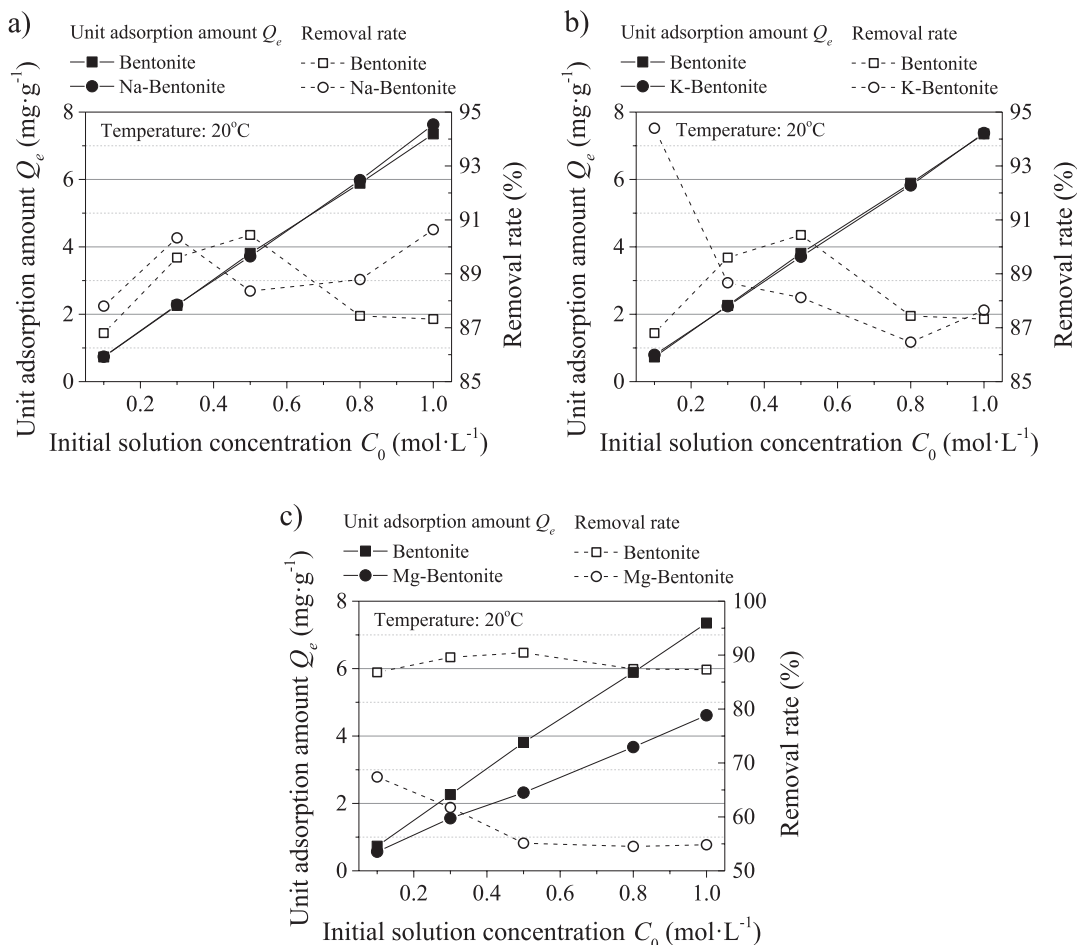


Fig. 1. Effect of initial solution concentration: a) Na-Bentonite, b) K-Bentonite, c) Mg-Bentonite.

## Results and Discussion

### Experiment Results

#### *Effect of Initial Concentration*

The effect of initial concentration is shown in Fig. 1, and these three figures are the comparison between three different kinds of modified bentonite and unmodified bentonite, respectively. With the increase of the initial solution concentration, the unit adsorption capacity  $Q_e$  also increased, and increased singly in the five groups of experimental data. It can be seen from the figure that the unit adsorption capacity of Na-Bentonite is the highest and the growth rate is the largest, the adsorption amount is more than 2 mg/g at the optimal removal rate over 90% when the solution concentration is  $0.3 \text{ mol}\cdot\text{L}^{-1}$ . The adsorption effect of Na-Bentonite is also better than that of unmodified Bentonite, but the performance is quite similar. However, the adsorption effect of Mg-bentonite is relatively poor, which may be due to the silicon aluminum ratio of the original bentonite is not improved in the modification process of Mg-Bentonite, which also makes the weak attraction of the modified bentonite to metal cations and thus the adsorption effect decreased [15, 34].

In terms of adsorption rate, Na-Bentonite shows relatively stable adsorption rate under the condition of high initial concentration, while the K-Bentonite depicts a decreasing trend with the concentration increase. The adsorption rate of unmodified Bentonite decreases with the increase of initial solution concentration, which indicates that higher pollutant concentration is easy to inhibit the adsorption reaction. The adsorption rates of Na and K-Bentonite are generally kept within the floating range of 10% up and down, which shows that the modified bentonite is less sensitive to the concentration of solution, and the adsorption of cesium does not affect the surface adsorption activity, thus the purpose of modification can be achieved. The removal rate of Mg-Bentonite is unsatisfactory, with the figure around 55%. And it comes to be stable and not sensitive to the concentration, which is lower than that of unmodified Bentonite, and its adsorption characteristics for cations are weaker than the other two modified bentonites [35]. Some other scholars have researched on cesium sorption via different materials, also some

other researches had been taken on the sorption reaction based on bentonite or modified bentonite composite. The comparison of various sorbents to investigate the effect of initial solution concentration is listed in Table 1. It is consistent that the sorption rate decreases with the increase of solution concentration, regardless of the optimal value of Bentonite and Na-Bentonite in Fig. 1 [36, 37]. Further, the sorption performance of bio sorbent seems not to be satisfactory. And the sorption capacity of Polymer composites may be reinforced with the increase of initial solution concentration [38, 39]. The decrease trend of bentonite sorption may be influenced by the acidity of solution, which caused by the solution concentration and sorption reaction.

#### *Effect of Sorbent Dosage*

Fig. 2 depicts the effect of bentonite dosage during adsorption process. Similarly, the unit adsorption amount of the four materials decreased with the increase of the bentonite dosage. The highest unit adsorption capacity of Na-Bentonite appears at the dosage of 1.0 g, while the remaining three groups of optimal values appear when the dosage is 1.0 g too. The Na-Bentonite presents similar adsorption capacity with the unmodified bentonite, while the K-Bentonite is just a little bit better. The sorption points in these three sorbents are similar, but the Mg-Bentonite is 25% adsorption capacity lower. This may be caused by the fewer sorption site on the surface or the active sorption point on cesium may be blocked. The activity of Na and K ions cover the surface at a higher concentration in the solution, thus promoting the adsorption of cesium ions [16].

The results of adsorption rate are similar to the test results of unit adsorption capacity. The adsorption capacity of Na-Bentonite and unmodified Bentonite is around 90%, but the unmodified Bentonite depicts more stable and higher removal rate. The adsorption rate of K-Bentonite is similar with unmodified Bentonite, and a constant increase with the adding of dosage can be witnessed [40, 41]. The adsorption rate of Mg-Bentonite is lower than 80%, while the changing trend is similar to that of Na-Bentonite. With the increase of bentonite dosage, the adsorption rate increases, and the increase percent can be ignored when it's over 2.0 g. In terms of dosage, Na-Bentonite and K-Bentonite is

Table 1. Sorption performance comparison of various sorbents under initial concentration.

Type of sorbent	Sorbent	Optimal initial solution concentration	Sorption rate	Reference
Inorganic	Bentonite	100~500 mg/L	Decrease	[15]
	Bentonite	100~500 mg/L	Decrease	[46]
	Ferrite	0.001~0.1 mol/L	Decrease	[39]
Bio	Azolla filiculoides	25~600 mg/L	68%	[43]
Polymer composites	ZrP-AMP	$3.76.0\times 10^{-5}\sim 7.52\times 10^{-3} \text{ M}$	4~96%	[40]

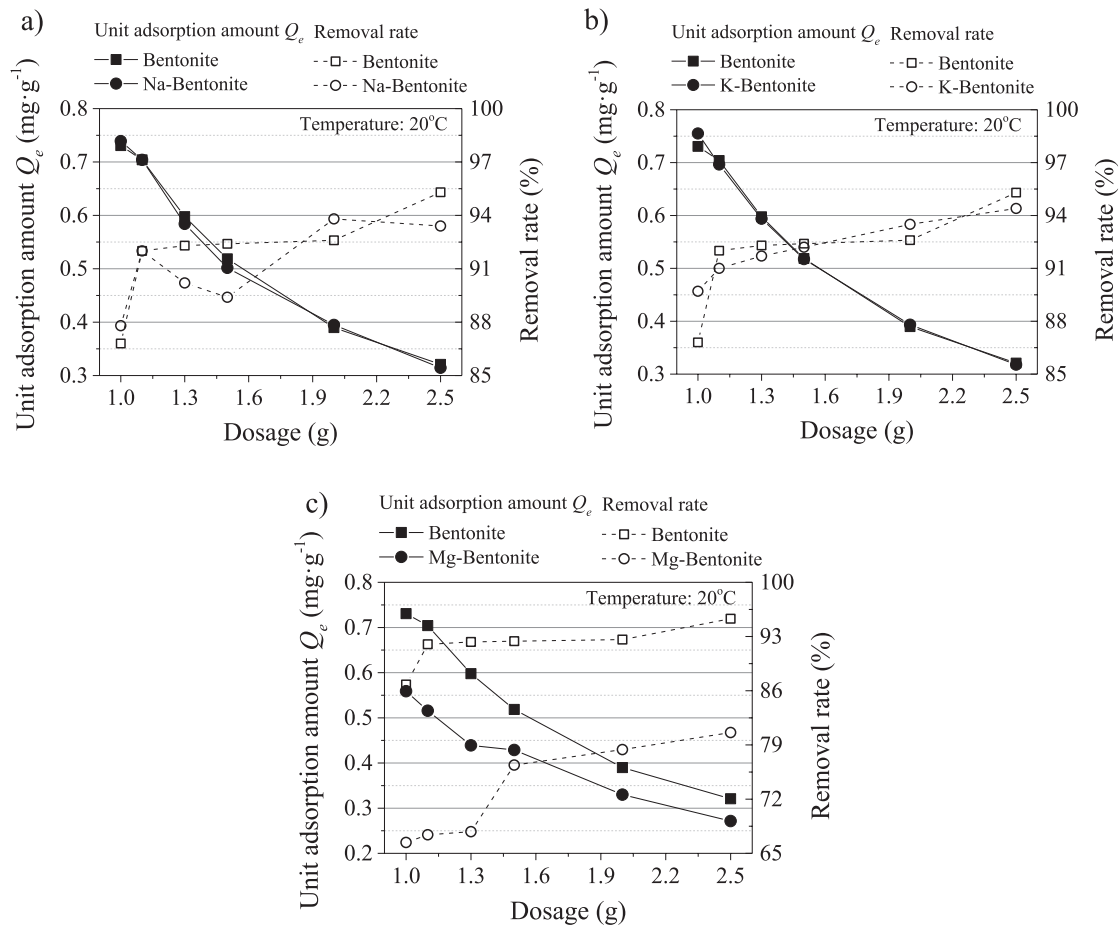


Fig. 2. Effect of bentonite dosage: a) Na-Bentonite, b) K-Bentonite, c) Mg-Bentonite.

Table 2. Sorption performance comparison of various sorbents under sorbent dosage.

Type of sorbent	Sorbent	Sorbent dosage	Sorption rate	Reference
Inorganic	Bentonite	20~100 mg	30~99%	[15]
	Bentonite	0.25~5 g	Decrease	[46]
Composite	nZVI-Z	1~10 g/L	7.82%~64.54%	[36]
	nFe/Cu-Z	1~10 g/L	19.91~73.72%	

relatively stable, Mg-Bentonite presents poor adsorption performance and that is the worst. The comparison of composite and bentonite under sorbent dosage is listed in Table 2. The sorption rate is below 80%, 20% lower than bentonite. It indicates the similar trend with Table 1, but the composites of ZVI (zero valent iron) and Fe/Cu are in increasing trend with the increase dosage of sorbent [42]. It is easy to know that, the increase of metal composite sorbent provides much more surface area and sorption site, which active the reaction points.

*Effect of pH*

The effect of solution pH is shown in Fig. 3. In this section, pH 3.0, pH 7.0 and pH 11.0 were

chosen to present the acidic, neutral and alkaline environment. It can be seen from the figure that the adsorption characteristics of Na-Bentonite under three different acid-base environments are the most stable, regardless of the better performance in alkaline solution. The adsorption effect of Na-Bentonite and K-Bentonite under alkaline conditions is better than that of unmodified Bentonite, while in acidic situation, the K-Bentonite and Mg-Bentonite present poor adsorption performance with the unit adsorption amount lower than 0.5 mg/g. The Mg-Bentonite is not varying from acidic to alkaline, but the ion exchange reaction may be blocked on the surface [43, 44]. Generally speaking, the adsorption effect of bentonite on cesium is relatively dull under neutral and acidic conditions. From the unit adsorption capacity in neutral to acidic environment, it

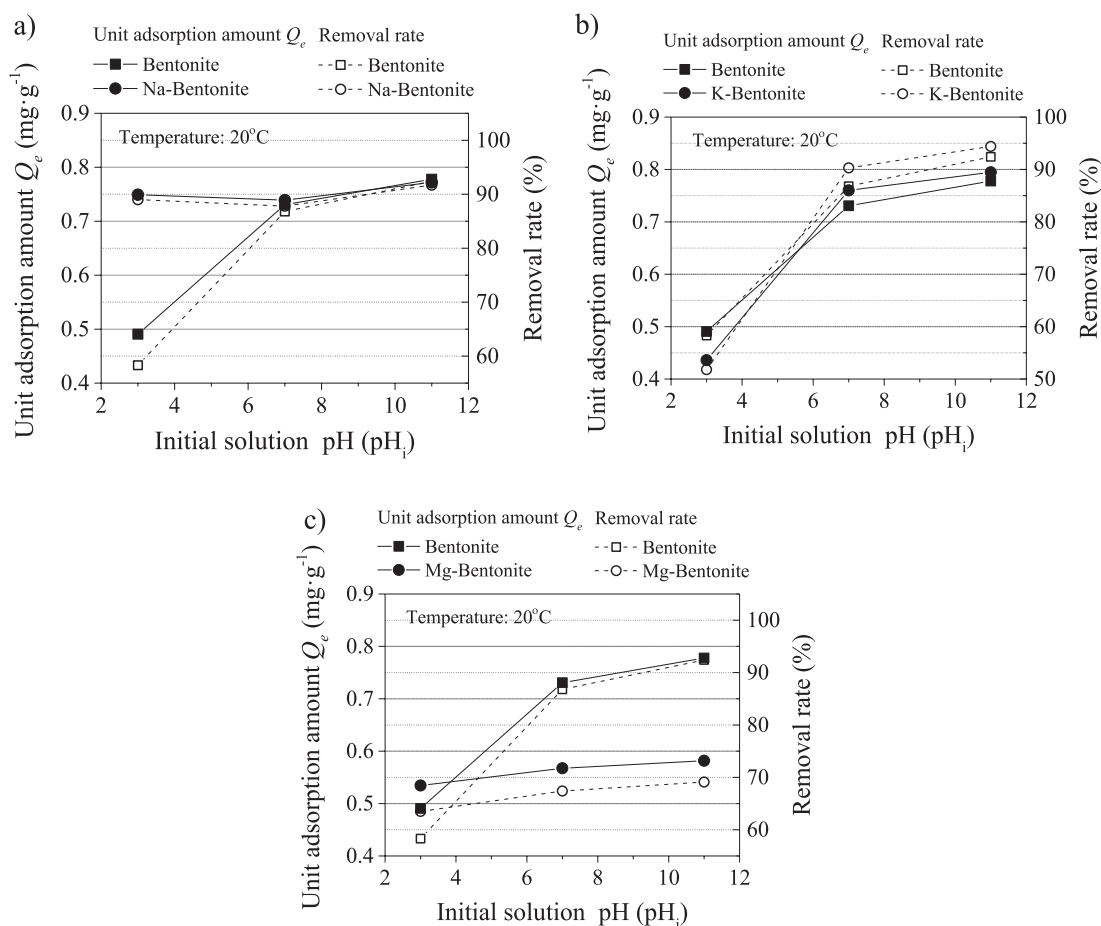


Fig. 3. Effect of solution pH: a) Na-Bentonite, b) K-Bentonite, c) Mg-Bentonite.

Table 3. Sorption performance comparison of various sorbents under pH.

Type of sorbent	Sorbent	Solution pH	Sorption rate	Reference
Inorganic	Bentonite	8-10 (Optimal)	90%	[15]
	Bentonite	8-11 (Optimal)	Increase	[46]
	Zeolite	4-10	99%	[60]
Bio	O. basilicum seeds	1-7	48.14%	[44]
Polymer composites	ZrP-AMP	< 7	96%	[40]

can be seen that the change of pH from 3 to 7 makes tiny changing range of adsorption capacity. Under the extreme alkaline condition of pH 11, cesium adsorption was fully reacted. Under alkaline conditions, the more active metal cations are mixed in the solution, which intensifies the ion replacement [45, 46]. The lower adsorption capacity of Mg-Bentonite may be due to the inhibitory relationship between Na<sup>+</sup> or K<sup>+</sup> and Cs<sup>+</sup> in the solution, which reduces the adsorption activity on the bentonite surface and hinders the ion exchange reaction [47]. In terms of adsorption rate, the maximum adsorption rate of Na-Bentonite is up than 90%, while the adsorption rate of the other two groups of modified bentonites is lower, and not steady from acidic to

alkaline sorption environment. Table 3 illustrates the sorption performance comparison of various sorbents under different pH value. The inorganic sorbent present better sorption capacity in alkaline environment, while crystalline compound is much easier to form in pH value lower than 7 [48, 49].

#### Effect of Reaction Time

Five reaction time periods conducted in this paper, and the test results are depicted in Fig. 4. The unit adsorption capacity of Na-Bentonite is lower than that of unmodified Bentonite, and the unit adsorption capacity of K-Bentonite is relatively higher than that of

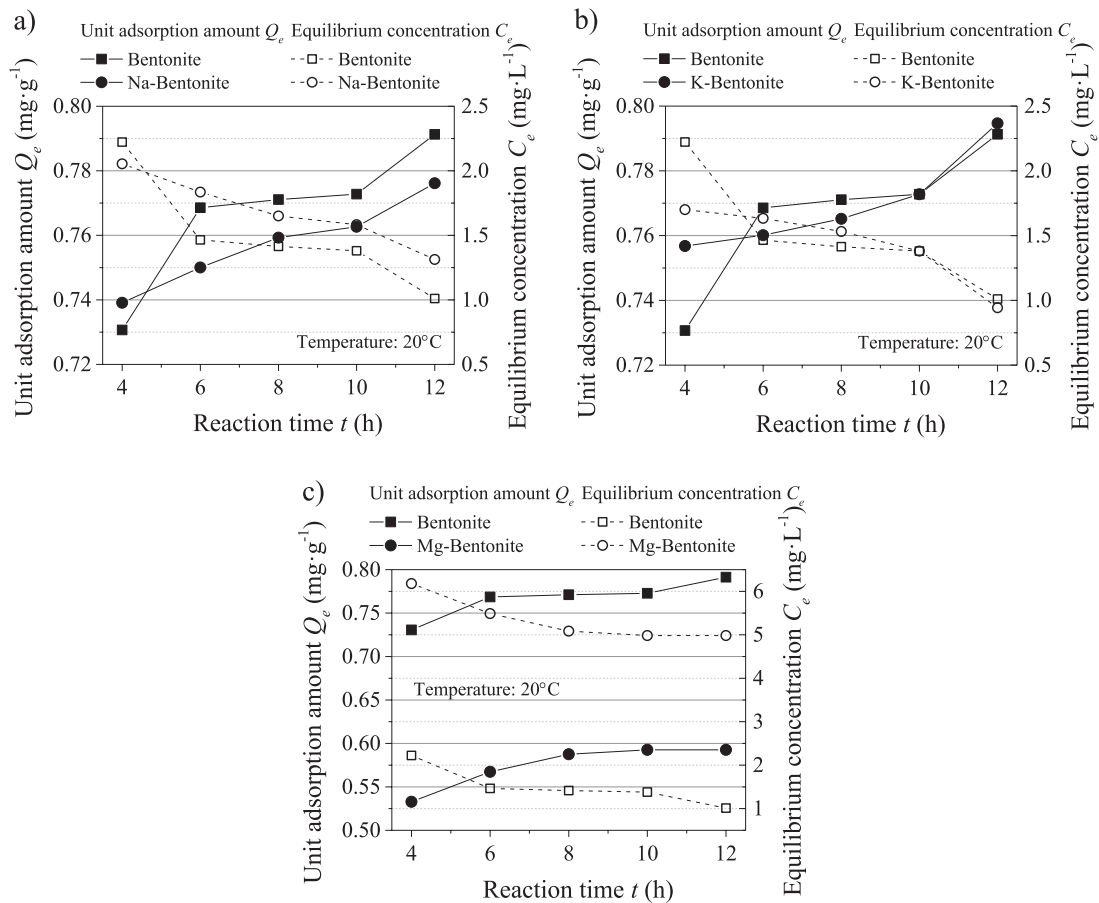


Fig. 4. Effect of reaction time: a) Na-Bentonite, b) K-Bentonite, c) Mg-Bentonite.

Table 4. Sorption performance comparison of various sorbents under reaction time.

Type of sorbent	Sorbent	Reaction time	Reference
Inorganic	Sericite	120 min	[52]
	Zeolite A	1.5~2 h	[53]
Bio	<i>O. basilicum</i> seed	30 min	[60]
	Activated carbon from almond shell	1 h	[55]
Polymer composites	Polyaniline titanotungstate	2 h	[56]
	Imprinted polymer	2 h	[43]

unmodified bentonite at 12 hours, and stays at a high level. It indicates that there is not enough active area on the surface of Mg-Bentonite to adsorb  $\text{Cs}^+$ . It can be seen from the figure that with the passage of time, the unit adsorption capacity changes little with time, but generally shows an upward trend [50]. On the contrary, the equilibrium concentration decreases with time, which indicates that the adsorption reaction of bentonite continues.

The adsorption effect of K-Bentonite was the best, and the equilibrium concentration decreased to  $1 \text{ mg}\cdot\text{L}^{-1}$  at 12 h. The adsorption effect of Mg-Bentonite is the worst. Similar to the previous description,

the equilibrium concentrations of Mg-Bentonite are higher than  $5 \text{ mg}\cdot\text{L}^{-1}$ . It can be seen that lower ionic activity compared with  $\text{Na}^+$  and  $\text{K}^+$  is not conducive to the adsorption of  $\text{Cs}^+$ . On the contrary, it will inhibit the adsorption reaction. The surface activity of Mg-Bentonite is significantly lower than that of the other two groups of modified bentonites [51].

The comparison between various sorbents under the change of sorption time is shown in Table 4. It seems that the Bentonite investigated in this paper took far more time in cesium adsorption. And the bio sorbents and polymer composites may take fewer reaction time to meet the equilibrium [52-56].

Effect of Temperature

The effect of temperature in this test is to investigate the promotion or inhibition of temperature on adsorption reaction. The results of temperature effect are shown in Fig. 5, which is basically consistent with the results of reaction time. The unit adsorption capacity of Mg-Bentonite is lower than that of natural bentonite, but it is not seriously affected by the increase of temperature. When the temperature changes from 60°C to 80°C, the adsorption capacity decreases sharply in Na-Bentonite and Mg-Bentonite. The adsorption capacity of Na-Bentonite and K-Bentonite is also greatly affected by temperature, while Na-Bentonite is slightly affected by temperature. In the range of 60°C to 80°C, the adsorption capacity of Na-Bentonite witnessed almost no decrease, while that of

Na-Bentonite decreases by nearly 5%. Although the maximum unit adsorption capacity of Na-Bentonite and K-Bentonite reached 0.76 mg/g, it continued to decline under the influence of temperature and was lower than that of unmodified Bentonite. The law of equilibrium concentration is similar, and the modified bentonite seems to be more sensitive to the pH value [57]. In general, the ion change may be influenced by the temperature, especially in active anions, that is why 20°C was selected as the test parameters.

Based on the above experimental data, it can be concluded that both unmodified Bentonite and modified bentonites possess prominent attraction characteristics to cesium ions in solution. The preference of bentonite for Na<sup>+</sup>, K<sup>+</sup>, Mg<sup>2+</sup> can be obtained from the test results under the influence of different parameters, and the overall ranking is: Cs<sup>+</sup>>Mg<sup>2+</sup>>Na<sup>+</sup>≥K<sup>+</sup> [58, 59]. The different

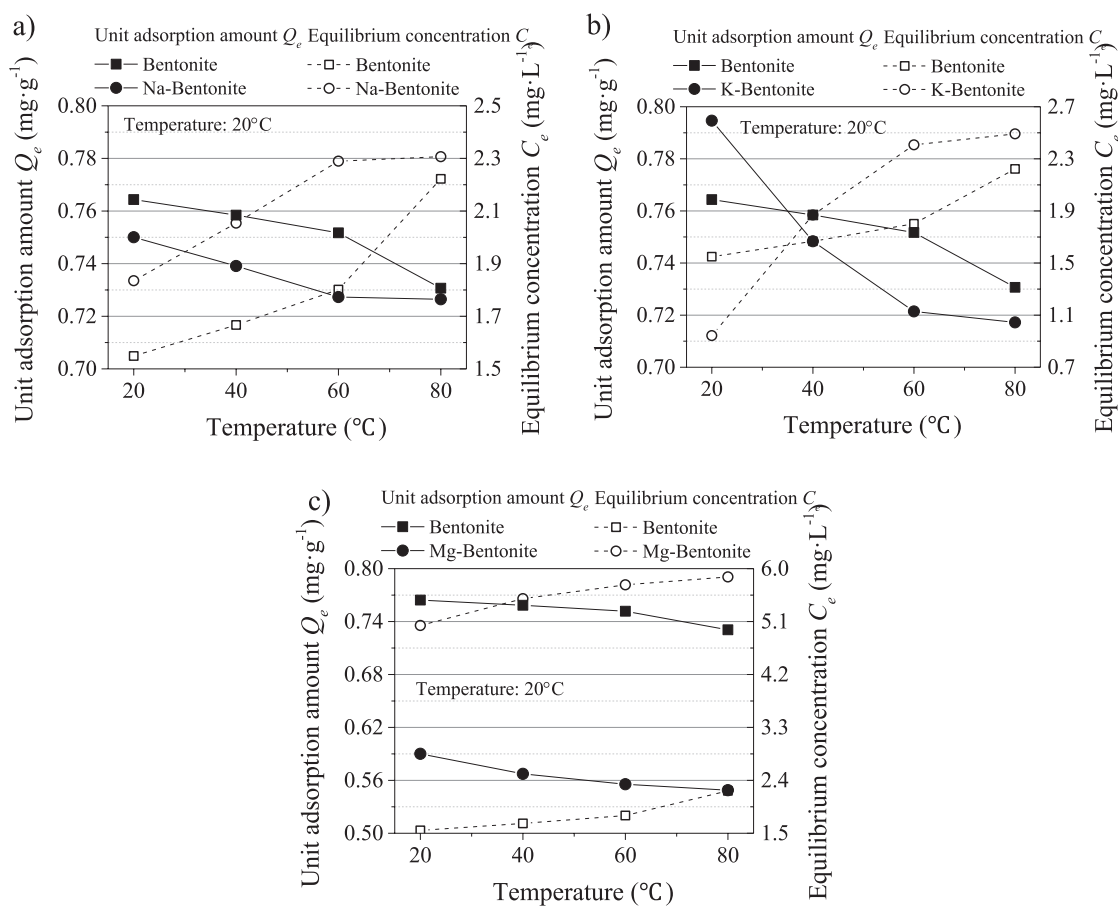


Fig. 5. Effect of temperature: a) Na-Bentonite, b) K-Bentonite, c) Mg-Bentonite.

Table 5. Sorption performance comparison of various sorbents under temperature.

Type of sorbent	Sorbent	Temperature	Sorption capacity	Reference
Inorganic	Bentonite	292K~312 K	20.2 mg/g	[15]
	Sericite	288~318 K	6.68 mg/g	[52]
	Analcime from fly ash	287~307 K	93 mg/g	[60]
	Metal hexacyanoferrate-prepared sorbents	305~335 K	98.25 mg/g	[5]

reaction temperature of various sorbents is shown in Table 5. The temperature value is similar in natural material or modified natural sorbents, which is around 300 K.

Adsorption Isotherms

Based on the test results in effect of initial concentrations, three different isothermal adsorption models were fitted in this section. The fitting curve is shown in Fig. 6, and they were fitted in Langmuir isothermal model, Freundlich isothermal model and Redlich-Peterson isothermal model respectively. It can be seen from the data fitting in the figure that the fitting degree of the three models is relatively high, and the R-P model is an improvement of the traditional

model, which is reflected in the higher curvature and smoothness of the curve.

The detailed fitting parameters for cesium adsorption is shown in Table 6.  $R^2$  reflects the fitting degree of the curve, and the fitting  $R^2$  of R-P model based on four groups of bentonite test data is higher than 0.990.

Therefore, the R-P model represents the best fitting, compared with other two conventional models. In Freundlich isothermal model, the value of  $n$  between 1.5 to 3.0 indicates better reaction environment for cesium adsorption. In this paper, the  $n$  is in this range, and the first three  $1/n$  is below 0.500, which indicates that the ion exchange reaction is easy to occur. However, the lower of  $1/n$  also means better adsorption, and in Table 6. the Mg-Bentonite possesses the poorest adsorption performance with the  $1/n$  of 0.604. Further, the fitting

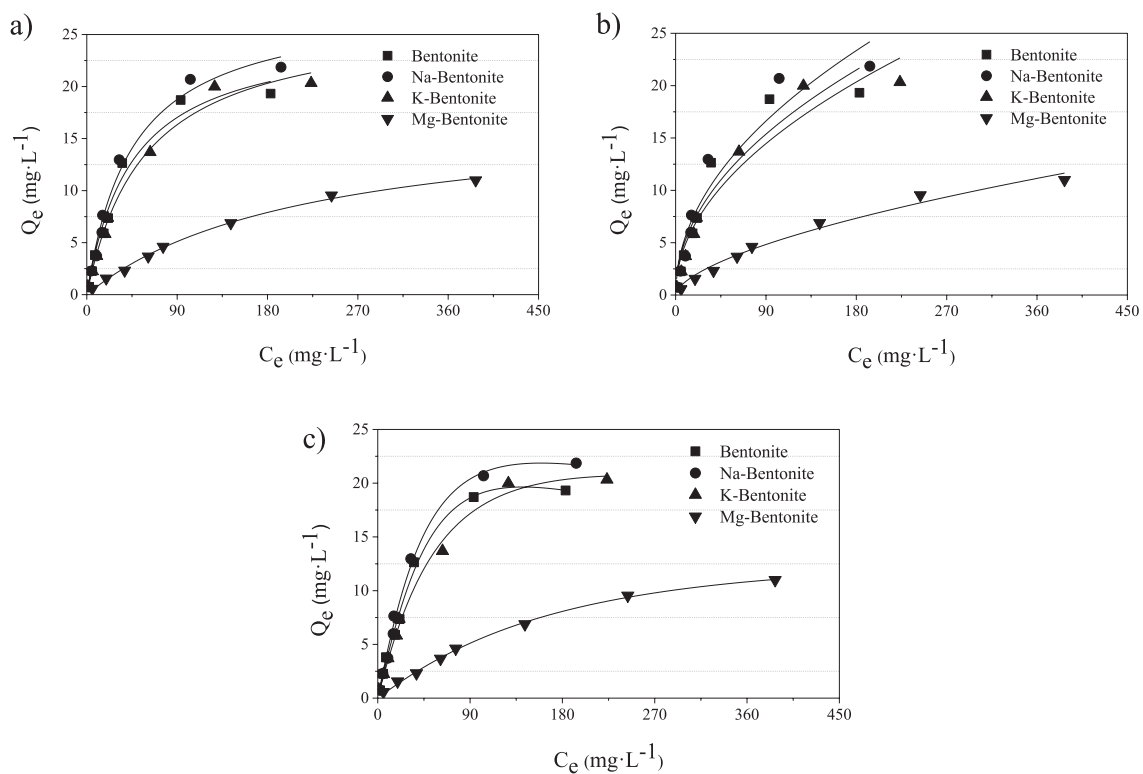


Fig. 6. Isothermal model for cesium adsorption: a) Langmuir isothermal model, b) Freundlich isothermal model, c) Redlich-Peterson isothermal model.

Table 6. Isothermal model parameters for cesium adsorption.

Model	Langmuir isothermal model			Freundlich isothermal model		Redlich-Peterson isothermal model				
	$Q_m$ (mg/g)	$K_L$	$R^2$	$K$ (mg/g)	$1/n$	$R^2$	$K_{RP}$ (L/g)	$a_{RP}$ (L/mg)	$\beta$	$R^2$
Bentonite	25.513	0.022	0.975	1.738	0.484	0.901	0.419	0.001	1.50	0.993
Na- Bentonite	28.225	0.022	0.982	1.826	0.491	0.916	0.486	0.002	1.39	0.993
K- Bentonite	26.843	0.017	0.988	1.573	0.493	0.943	0.373	0.003	1.27	0.992
Mg- Bentonite	17.486	0.004	0.996	0.319	0.604	0.979	0.071	0.001	1.23	0.997

of Langmuir isothermal model is better than Freundlich isothermal model. It means that the binding energy on the whole surface is uniform, and the adsorption is more likely to be monolayer adsorption [60]. From Langmuir isothermal model, the best adsorption capacity is witnessed in Na-Bentonite with the  $Q_m$  of 28.225 mg/g, which is comprehensive compared with other research [61, 62]. It also can be seen that the K-Bentonite present better performance than unmodified bentonite, even though it is 7% lower than Na-Bentonite.

Adsorption Kinetics

Based on the test results in effect of reaction time, three different kinetic adsorption models were fitted in

this section. The fitting curve is shown in Fig. 7, and they illustrate Pseudo-first-order kinetic model, Pseudo-second-order kinetic model and Intragranular diffusion model respectively. Different from the Isotherm models, the fitting degree in this part is not comprehensive. This figure depicts that Pseudo-second-order kinetic model represents better fitting curve compared with Pseudo-first-order kinetic model and Intragranular diffusion model.

The Kinetic model parameters for cesium adsorption are shown in Table 7. In this table, the equilibrium adsorption capacity in Pseudo-second-order kinetic model (16.32, 15.75, 15.94 and 12.72 mg/g) is relatively higher than the Pseudo-first-order model (15.61, 15.29, 15.50 and 11.86 mg/g).

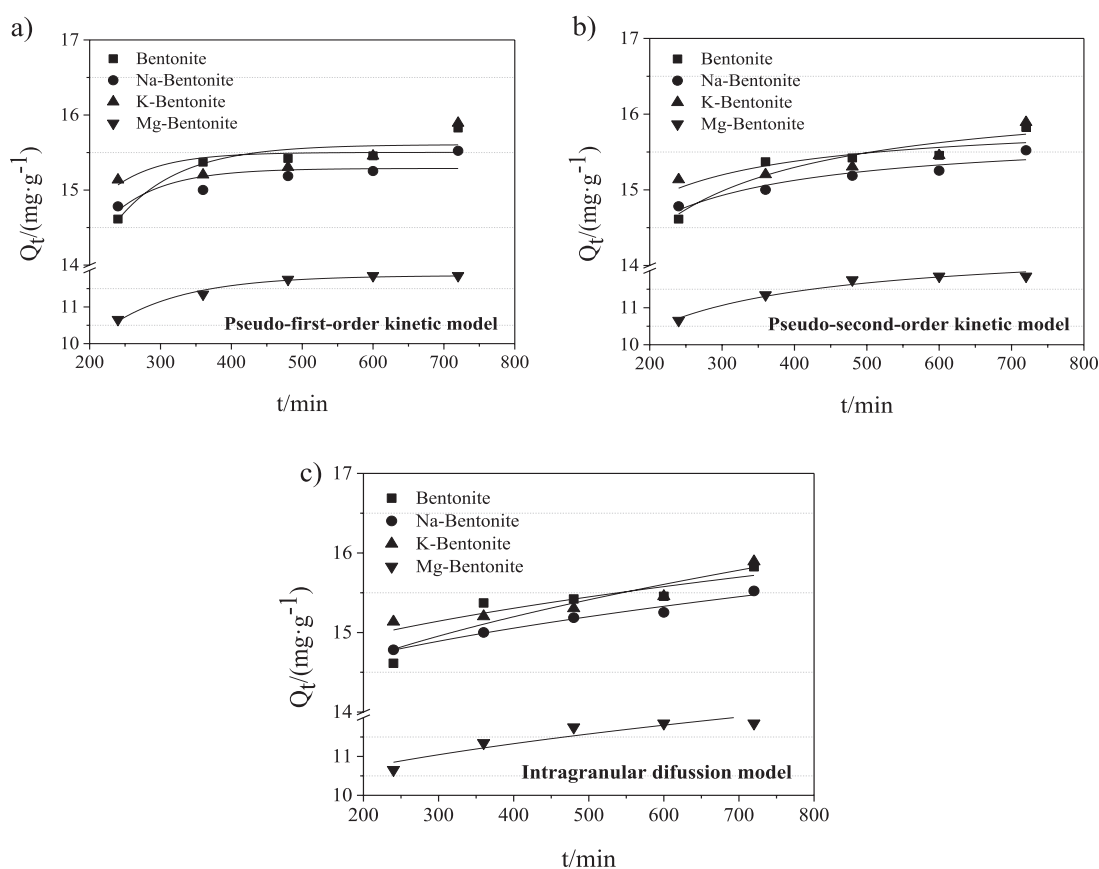


Fig. 7. Kinetic model for cesium adsorption: a) Pseudo-first-order kinetic model, b) Pseudo-second-order kinetic model, c) Intragranular diffusion model

Table 7. Kinetic model parameters for cesium adsorption.

Model	Pseudo-first-order kinetic model			Pseudo-second-order kinetic model			Intragranular diffusion model		
	$k_1$ (mg/g)	$Q_e$ (mg/g)	$R^2$	$k_2$ (g/mg·min)	$Q_e$ (mg/g)	$R^2$	$k_{int}$ (g/mg·min <sup>1/2</sup> )	$C$ (mg/g)	$R^2$
Bentonite	0.0114	15.61	0.859	0.0023	16.32	0.872	0.091	13.39	0.784
Na-Bentonite	0.0138	15.29	0.575	0.0038	15.75	0.877	0.061	13.83	0.963
K-Bentonite	0.0149	15.50	0.502	0.0043	15.94	0.899	0.061	14.09	0.740
Mg-Bentonite	0.0094	11.86	0.980	0.0018	12.72	0.957	0.106	9.21	0.815

The fitting of Pseudo-first-order kinetic model seems not to be satisfactory, and the adsorption seems to be consistent through the whole process under the fitting of Pseudo-second-order kinetic model. From the  $k_2$ , the unmodified bentonite presents the lowest, which means better ion exchange reaction. The hinder of Na-Bentonite ion exchange may be influenced by the origin content of Na in bentonite [63]. Otherwise, the whole adsorption process is well fitted to the intragranular diffusion model, which means that the reaction is in the form of both physical and chemical adsorption, combined with intragranular delivery

#### *Sorbents Micro-Scope Characterization*

In order to further study the mechanism of  $\text{Cs}^+$  adsorption by bentonite, the Fig. 8 is the SEM images. By comparing the images before and after the reaction, it can be found that the crystal structure before the reaction is clear and the surface is smooth and flat. After the reaction, the crystal structure of bentonite surface changed, and cesium was adsorbed on the surface to form a fine flocculent film, that means agglomerates on the surface. The surface was loose before adsorption, but to be consistent after adsorption because the voids were reduced and small particles emerged on the

surface. The surface crystal structure of Na-Bentonite is complex and diverse. In addition, the pore size in channels and pore cavity of modified bentonite is larger than that of unmodified Bentonite, which makes the radius of hydrated ions of adsorbed ions smaller than pores, thus to obtain better adsorption performance [64, 65]. The modification of bentonite by inorganic acid effectively expands the internal pores and is conducive to the promotion of adsorption reaction. When the pore size of bentonite is tiny, the reaction is tended to terminate quickly, which is not conducive to the steady decline of equilibrium concentration.

Fig. 9 depicts the XRD pattern of bentonite after adsorption process. The Fig. 9b) is a sketch of sorption process. As shown in Fig. 9a), the components before and after adsorption is almost no difference, which mostly composed of montmorillonite and quartz. The adsorption process and mechanism can be referred to the change of Al-O-Si and Si-O-Si. Thus, the adsorption effect of bentonite mainly depends on two aspects. The first aspect is the internal pore size, which has been explained in Fig. 8. On the other hand, an essential factor is that aluminum in bentonite replaces the amount of silicon in silica tetrahedron in bentonite cell [66-68]. And that provided the cation exchange sites and ion exchange possibility. Besides of these, for more

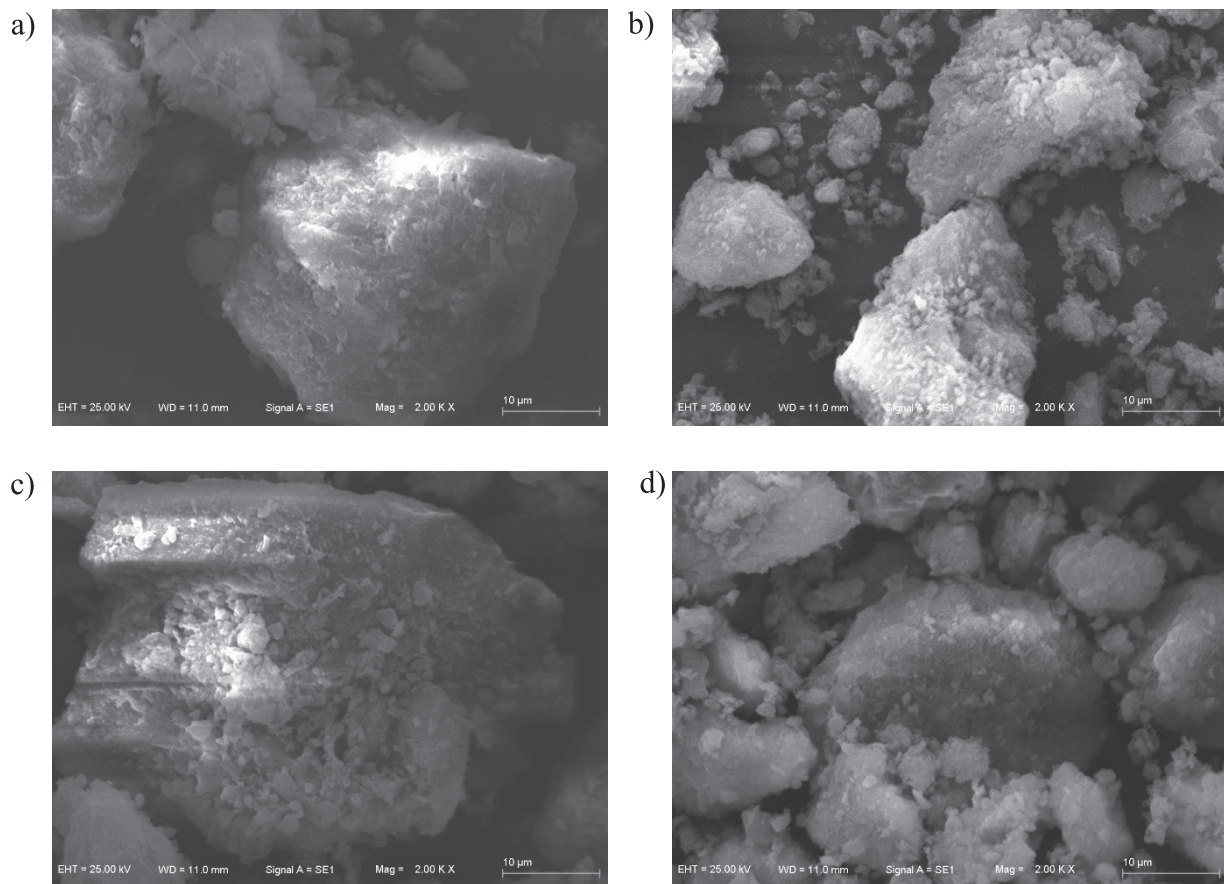


Fig. 8. SEM images on the surface of bentonite: a) Bentonite, before adsorption, b) Bentonite, after adsorption, c) Na- Bentonite, before adsorption, d) Na- Bentonite, after adsorption.

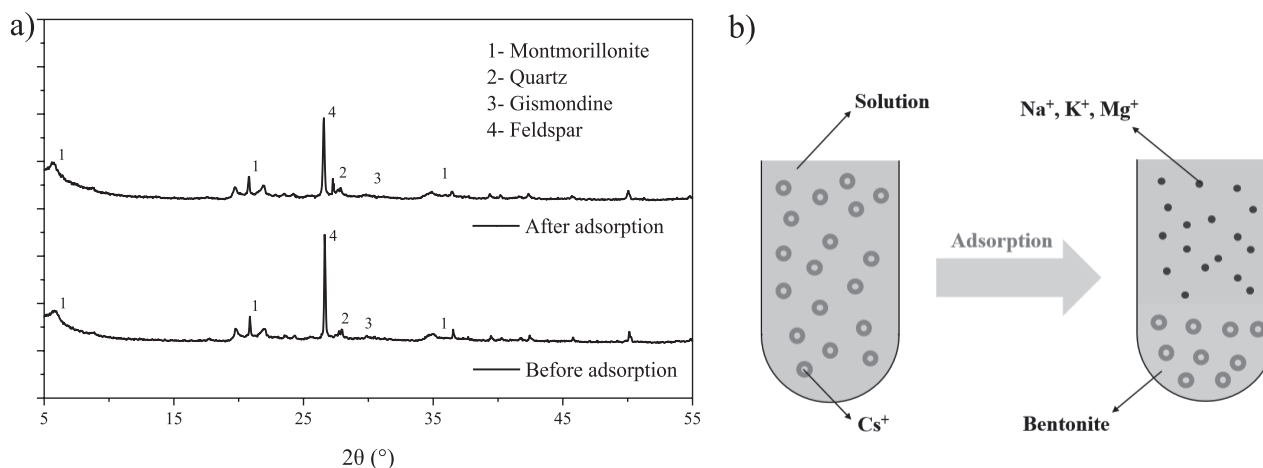


Fig. 9. XRD pattern and sketch of sorption process: a) XRD pattern of bentonite, b) Sketch of sorption process.

deeper research, BET (Specific surface area test), FTIR (Fourier Transform Infrared Spectroscopy) combined with some other methods will be conducted in future studies.

### Conclusion

This paper investigated the adsorption tests via unmodified Bentonite (Bentonite) and three different kinds of modified bentonite (Na-Bentonite, K-Bentonite and Mg-Bentonite). Various affecting parameters, containing dosage of bentonite, initial concentration of solution, pH value (Acid-base environment), reaction time and temperature, were conducted and analyzed in adsorption experiments. The SEM and XRD tests were also conducted for micro-scope insight into adsorption mechanism. The results can be concluded as below:

(1) The modified bentonite can be utilized as effective adsorbent for cesium contaminated waste. According to the test results, by using 1.1 g bentonite dosage and 1.0 mol/L solution concentration, the Na-Bentonite plays significant adsorption capacity. It is indicated that the maximum adsorption rate is 95.30% under alkaline environment, which prompt the adsorption reaction.

(2) The Langmuir isothermal model and Intragranular diffusion kinetic model fit the test data well, which means that monolayer adsorption takes place, while both physical and chemical adsorption reaction combing with intragranular delivery affected between the diffuse double layer. The maximum adsorption capacity of modified bentonite was predicted to be approximately 28.2 mg/g, as an excellent adsorption capacity comparing with other research.

(3) The unspecific sorption and precipitation mechanism increase the thickness of double layer, of which the capacity strongly affected by specific surface area and microscopic atomic size. The overall ranking of attraction between bentonite and ions is:  $Cs^+ > Mg^{2+} > Na^+ \geq K^+$ . The internal pore size on the surface of bentonite and the amount of aluminum replaces

silicon in silica tetrahedron in bentonite cell, are the two main factors of the bentonite adsorption performance.

### Acknowledgments

The research presented here is supported by the National Natural Science Foundation of China (52078317), Natural Science Foundation of Jiangsu Province for Excellent Young Scholars (BK20211597), project from Bureau of Housing and Urban-Rural Development of Suzhou (2021-25; 2021ZD02; 2021ZD30), Bureau of Geology and Mineral Exploration of Jiangsu (2021KY06), China Tiesiju Civil Engineering Group (2021-19), CCCC First Highway Engineering Group Company Limited (KJYF-2021-B-19) and CCCC Tunnel Engineering Company Limited (8gs-2021-04).

### Conflict of Interest

The authors declare that they have no conflicts of interest.

### References

1. WISSOCQ A., BEUCAIRE C., LATRILLE C. Application of the multi-site ion exchanger model to the sorption of Sr and Cs on natural clayey sandstone. *Applied Geochemistry*, **93**, 167, **2018**.
2. KRUPSKAYA V., NOVIKOVA L., TYUPINA E., BELOUSOV P., DORZHEVA O., ZAKUSIN S., KIM K., ROESSNER F., BADETTI E., BRUNELLI A., BELCHINSKAYA L. The influence of acid modification on the structure of montmorillonites and surface properties of bentonites. *Applied Clay Science*, **172**, 1, **2019**.
3. ELJAMA O., SHUBAIR T., TAHARA A., SUGIHARA Y., MATSUNAGA N. Iron based nanoparticles-zeolite composites for the removal of cesium from aqueous solutions. *Journal of Molecular Liquids*, **277**, 613, **2019**.

4. SAITO Y., SHIMIZU S., KUMAGAI S., KAMEDA T., YOSHIOKA T. Removal of cesium ions from A-type zeolites using sodium tetrakis (4-fluorophenyl) borate and sodium tetraphenyl borate. *Journal of Radioanalytical and Nuclear Chemistry*, **327** (1), 337, **2021**.
5. GASSER M.S., ALY M.I., ALY H.F. Selective removal of cesium ions from aqueous solutions using different inorganic metal hexacyanoferrate-prepared sorbents. *Particulate Science and Technology*, **37** (4), 464, **2017**.
6. GALAMBOS M., KUFCAKOVA J., RAJEC P. Adsorption of cesium on domestic bentonites. *Journal of Radioanalytical and Nuclear Chemistry*, **281** (3), 485, **2009**.
7. TANG Q., TANG X.W., LI Z.Z., WANG Y., HU M.M., ZHANG X.J., CHEN Y.M. Zn(II) Removal with Activated Firmiana Simplex Leaf: Kinetics and Equilibrium Studies. *Journal of Environmental Engineering (ASCE)*, **138** (2), 190, **2012**.
8. AKCANCA F., AYTEKIN M. Impact of wetting-drying cycles on the hydraulic conductivity of liners made of lime-stabilized sand bentonite mixtures for sanitary landfills. *Environmental Earth Sciences*, **72** (1), 59, **2014**.
9. TSUCHIDA T., MURAKAMI H., KURIHARA O., ATHAPATHTHU A.M.R.G., TANAKA Y., UENO K. Geotechnical sealing material for coastal disposal facility for soils and wastes contaminated by radioactive cesium. *Marine Georesources & Geotechnology*, **35** (4), 481, **2017**.
10. ZHAO R., LI M., MA S.D., YANG T.X., JING L.Y. Material selection for landfill leachate piping by using a grey target decision-making approach. *Environmental Science and Pollution Research*, **28** (1), 494, **2012**.
11. ABDEL-KARIM A.A.M., ZAKI A.A., ELWAN W., EL-NAGGAR M.R., GOUDA M.M. Experimental and modeling investigations of cesium and strontium adsorption onto clay of radioactive waste disposal. *Applied Clay Science*, **132**, 391, **2016**.
12. ZHAO R., XI B.D., LIU Y.Y., SU J., LIU S.L. Economic potential of leachate evaporation by using landfill gas: A system dynamics approach. *Conservation and Recycling*, **124**, 74, **2017**.
13. TANG Q., LIU W., LI Z.Z., WANG Y., TANG X.W. Removal of Aqueous Cu(II) with Natural Kaolin: Kinetics and Equilibrium Studies. *Environmental Engineering and Management Journal*, **17** (2), 467, **2018**.
14. BOURAIE E., MASOUD M. Adsorption of phosphate ions from aqueous solution by modified bentonite with magnesium hydroxide Mg (OH)<sub>2</sub>. *Applied Clay Science*, **140**, 157, **2017**.
15. CHANG Y.S., AU P.I., MUBARAK N.M., KHALID M., JAGADISH P., WALVEKAR R., ABDULLAH E.C. Adsorption of Cu(II) and Ni(II) ions from wastewater onto bentonite and bentonite/GO composite. *Environmental Science and Pollution Research*, **27** (26), 33270, **2020**.
16. PARAB H., MAHADIK P., SENGUPT P., VISHWANADH B., KUMAR S.D. A comparative study on native and gamma irradiated bentonite for cesium ion uptake. *Progress in Nuclear Energy*, **127**, **2020**.
17. KOMINE H. Theoretical equations on hydraulic conductivities of bentonite-based buffer and backfill for underground disposal of radioactive wastes. *Journal of Geotechnical and Geoenvironmental Engineering*, **134** (4), 497, **2008**.
18. KOMINE H., OGATA N. Experimental study on swelling characteristics of sand-bentonite mixture for nuclear waste disposal. *Soils and Foundations*, **39** (2), 83, **1999**.
19. MIAH MUHAMMED YUSUF., VOLCHEK KONSTANTIN., KUANG WENXING., TEZEL F. Handan. Kinetic and equilibrium studies of cesium adsorption on ceiling tiles from aqueous solutions. *Journal of Hazardous Materials*, **183**, 712, **2010**.
20. VOLCHEK KONSTANTIN., MIAH MUHAMMED YUSUF., KUANG WENXING., DEMALEKI ZACK., TEZEL F. HANDAN. Adsorption of cesium on cement mortar from aqueous solutions. *Journal of Hazardous Materials*, **194**, 331, **2011**.
21. TANG Q., CHU J.M., WANG Y., ZHOU T., LIU Y. Characteristics and factors influencing Pb(II) desorption from a Chinese clay by citric acid. *Separation Science and Technology*, **51** (17), 2734, **2016**.
22. ZHAO R., ZHOU X., HAN J.J., LIU C.L. For the sustainable performance of the carbon reduction labeling policies under an evolutionary game simulation. *Technological Forecasting and Social Change*, **112**, 262, **2016**.
23. TANG Q., ZHOU T., GU F., WANG Y., CHU J.M. Removal of Cd(II) and Pb(II) from soil through desorption using citric acid: kinetic and equilibrium studies. *Journal of Central South University*, **24** (9), 1941, **2017**.
24. TANG Q., SHI P.X., YUAN Z., SHI S.J., XU X.J., KATSUMI T., Potential of zero-valent iron in remediation of Cd(II) contaminated soil: from laboratory experiment, mechanism study to field application. *Soils and Foundations (JGS)*, **59**, 2099, **2019**.
25. OFOMAJA A.E., PHOLOS I. A., NAIDOO E.B. Kinetics and competitive modeling of cesium biosorption onto chemically modified pine cone powder. *Journal of The Taiwan Institute of Chemical Engineers*, **44** (6), 943, **2013**.
26. OZEROGLU C., DOGAN E., KECELI G. Investigation of Cs(I) adsorption on densely crosslinked poly (sodium methacrylate) from aqueous solutions. *Journal of Radioanalytical and Nuclear Chemistry*, **289** (2), 577, **2011**.
27. PARK Y., LEE Y.C., SHIN W.S., CHOI S.J. Removal of cobalt, strontium and cesium from radioactive laundry wastewater by ammonium molybdophosphate polyacrylonitrile (AMP-PAN). *Chemical Engineering Journal*, **162** (2), 685, **2010**.
28. MELKIOR T., YAHIAOUI S., MOTELLIER S., THOBY D., TEVISSSEN E. Cesium sorption and diffusion in Bure mudrock samples. *Applied Clay Science*, **29** (3), 172, **2005**.
29. LEE J.O., CHO W.J., CHOI H. Sorption of cesium and iodide ions onto KENTEX-bentonite. *Environmental Earth Sciences*, **70** (5), 2387, **2013**.
30. OLATUNJI M.A., KHANDAKAR M.U., MAHMUD H.N.M.E., AMIN Y.M. *RSC Advances*, **5** (88), 71658, **2015**.
31. TESSIER A., CAMPBELL P.G.C., BISSON M. Sequential extraction procedure for the speciation of particulate trace metals. *Analytical Chemistry*, **51** (7), 844, **1979**.
32. TANG Q., LIU W., WANG H.Y., CHENG R., QIAN Y.F. Membrane behavior of bentonite-amended Fukakusa clay in K, Na and Ca solutions. *Journal of Central South University*, **23** (12), 3122, **2016**.
33. PARK S.M., ALESSI D.S., BAEK K. Selective adsorption and irreversible fixation behavior of cesium onto 2:1 layered clay mineral: a mini review. *Journal of Hazardous Materials*, **369**, 569, **2019**.
34. VOKAL A., VOPALKA D., VECERNIK P. An approach for acquiring data for description of diffusion in safety assessment of radioactive waste repositories. *Journal*

- of Radioanalytical and Nuclear Chemistry, **286** (3), 751, **2010**.
35. TANG Q., WANG H.Y., TANG X.W., WANG Y. Removal of aqueous Ni(II) with carbonized leaf powder: kinetic and equilibrium studies, *Journal of Central South University*, **23** (4), 778, **2016**.
36. LIU H.J., XIE S.B., XIA L.S., TANG Q., KANG X., HUANG F. Study on adsorptive property of bentonite for cesium. *Environmental Earth Sciences*, **75** (2), 148, **2016**.
37. SHEHA R.R., METWALLY E. Equilibrium isotherm modeling of cesium adsorption onto magnetic materials. *Journal of Hazardous Materials*, **143** (1), 354, **2007**.
38. MASHKANI S.G., GHAZVINI P.T.M. Biotechnological potential of *Azolla filiculoides* for biosorption of Cs and Sr: Application of micro-PIXE for measurement of biosorption. *Bioresource Technology*, **100**, 1915, **2009**.
39. SHEHA R.R., METWALLY E. Equilibrium isotherm modeling of cesium adsorption onto magnetic materials. *Journal of Hazardous Materials*, **143**, 354, **2007**.
40. KREMLYAKOVA N.Y., KOMAREVSKY V.M. Sorption of alkaline and alkaline-earth radionuclides on zirconium phosphate sorbent Termoxid-3A from aqueous solution. *Journal of Radioanalytical and Nuclear Chemistry*, **218** (2), 197, **1997**.
41. KURIHARA O., TSUCHIDA T., TAKAHASHI G., KANG G., MURAKAMI H. Cesium-adsorption capacity and hydraulic conductivity of sealing geomaterial made with marine clay, bentonite, and zeolite. *Soils and Foundations*, **58** (5), 1173, **2018**.
42. TABELIN C.B., SASAKI R., IGARASHI T., PARK I., TAMOTO S., ARIMA T., ITO M., HIROYOSHI N. Simultaneous leaching of arsenite, arsenate, selenite and selenate, and their migration in tunnel-excavated sedimentary rocks: I. Column experiments under intermittent and unsaturated flow. *Chemosphere*, **186**, 558, **2017**.
43. MASHKANI S.G., GHAZVINI P.T.M. Biotechnological potential of *Azolla filiculoides* for biosorption of Cs and Sr: Application of micro-PIXE for measurement of biosorption. *Bioresource Technology*, **100**, 1915, **2009**.
44. DURRANT C.B., BEGG J.D., KERSTING A.B., ZAVARIN M. Cesium sorption reversibility and kinetics on illite, montmorillonite, and kaolinite. *Science of The Total Environment*, **610**, 511, **2018**.
45. PLOTZE M., KAHR G., STENGELE R.H. Alteration of clay minerals-gamma-irradiation effects on physicochemical properties. *Applied Clay Science*, **23** (1), 195, **2003**.
46. YAO F.Y., LIU G.W., JI Y.B., TONG W.J., DU X.Y., LI K.J., SHRESTHA A., MARTEK I. Evaluating the environmental impact of construction within the industrialized building process: a monetization and building information modelling approach. *International Journal of Environmental Research and Public Health*, **17** (22), **2020**.
47. TANG Q., GU F., ZHANG Y., ZHANG Y.Q., MO J.L. Impact of biological clogging on the barrier performance of landfill liners. *Journal of Environmental Management*, **222**, 44, **2018**.
48. CHAKRABORTY D., MAJI S., BANDYOPADHYAY A., BASU S. Biosorption of cesium-137 and strontium-90 by mucilaginous seeds of *Ocimum basilicum*. *Bioresource Technology*, **98** (15), 2949, **2007**.
49. KHANDAKER S., TOYOHARA Y., SAHA G.C., AWUAL M.R., KUB T. Development of synthetic zeolites from bio-slag for cesium adsorption: Kinetic, isotherm and thermodynamic studies. *Journal of Water Process Engineering*, **33**, 101055, **2022**.
50. TANG Q., GU F., GAO Y.F., INUI T., KATSUMI T. Desorption Characteristics of Cr(III), Mn(II) and Ni(II) in Contaminated Soil Using Citric Acid and Citric Acid Containing Wastewater. *Soils and Foundations*, **58**, 50, **2018**.
51. BELOUSOV P., SEMENKOVA A., EGOROVA T., ROMANCHUK A., ZAKUSIN S., OLGA D., EKATERINA T., YULIA I., INNA T., MICHAIL C., VICTORIA K. Cesium Sorption and Desorption on Glauconite, Bentonite, Zeolite and Diatomite. *Minerals*, **9** (10), 625, **2019**.
52. KIM J.O., LEE S.M., JEON C. Adsorption characteristics of sericite for cesium ions from an aqueous solution. *Chemical Engineering Research and Design*. **92**, 368, **2014**.
53. EL-KAMASH A.M. Evaluation of zeolite A for the sorptive removal of Cs<sup>+</sup> and Sr<sup>2+</sup> ions from aqueous solutions using batch and fixed bed column operations. *Journal of Hazardous Materials*, **151** (2), 432, **2008**.
54. HANAFI A. Adsorption of cesium, thallium, strontium and cobalt radionuclides using activated carbon. *Journal of Atomic and Molecular Sciences*, **1** (4), 292, **2010**.
55. EL-NAGGAR I.M., ZAKARIA E.S., ALI I.M., KALIL M., EL-SHAHAT M.F. Chemical studies on polyaniline titanotungstate and its uses to reduction cesium from solutions and polluted milk. *Journal of Environmental Radioactivity*, **112**, 108, **2012**.
56. ZHANG Z., XU X., YAN Y. Kinetic and thermodynamic analysis of selective adsorption of Cs(I) by a novel surface whisker-supported ion-imprinted polymer. *Desalination*, **263**, 97, **2010**.
57. TANG Q., ZHANG Y., GAO Y.F., GU F. Use of Cement-Chelated Solidified MSWI Fly Ash for Pavement Material: Mechanical and Environmental Evaluations, *Canadian Geotechnical Journal*, **54** (11), 1553, **2017**.
58. KRUPSKAYA V., ZAKUSIN S., TYUPINA E., DORZHIEVA O., ZHUKHLISTOV A., BELOUSOV P., TIMOFEEVA M. Experimental Study of Montmorillonite Structure and Transformation of Its Properties under Treatment with Inorganic Acid Solutions. *Minerals*, **7**, 49, **2017**.
59. LIU R.Y., ZOU L.X., HUANG Q., CAO X.H., YANG C. Synthesis of analcime from fly ash and its adsorption of Cs<sup>+</sup> in aqueous solution. *Journal of Radioanalytical and Nuclear Chemistry*, **329**, 103, **2021**.
60. KRUPSKAYA V.V., ZAKUSIN S.V., TYUPINA E.A., DORZHIEVA O.V. Transformation of structure and adsorption properties of montmorillonite under thermochemical treatment. *Geochemistry International*, **57** (3), 314, **2019**.
61. BAYULKEN S., BASETIN E., GULU K., APAK R. Investigation and Modeling of Cesium(I) Adsorption by Turkish Clays: Bentonite, Zeolite, Sepiolite, and Kaolinite. *Environmental Progress & Sustainable Energy*, **30** (1), 70, **2011**.
62. FUKUSHI K., SAKAI H., ITONO T., TAMURA A., ARAI S. Desorption of intrinsic cesium from smectite: Inhibitive effects of clay particle organization on cesium desorption. *Environmental Science & Technology*, **48** (18), 10743, **2014**.
63. FUKUSHI K., FUKIAGE T. Prediction of Intrinsic Cesium Desorption from Na-Smectite in Mixed Cation

- Solutions. *Environmental Science & Technology*, **49** (17), 10398, **2015**.
64. OKUMURA M., NAKAMURA H., MACHIDA M. Mechanism of strong affinity of clay minerals to radioactive cesium: first-principles calculation study for adsorption of cesium at frayed edge sites in muscovite. *Journal of The Physical Society of Japan*, **82** (3), **2013**.
65. BABAKI H., SALEM A., JAFARIZAD A. Kinetic model for the isothermal activation of bentonite by sulfuric acid. *Materials Chemistry and Physics*, **108** (2), 263, **2008**.
66. PENG W., LI H., LIU Y., SONG S. A review on heavy metal ions adsorption from water by graphene oxide and its composites. *Journal of Molecular Liquids*, **230**, 496, **2017**.
67. NEELAVENI M., KRISHNAN P.S., RAMYA R., THERES G.S., SHANTHI K. Montmorillonite/graphene oxide nanocomposite as superior adsorbent for the adsorption of rhodamine B and nickel ion in binary system. *Advanced Powder Technology*, **30** (3), 596, **2019**.
68. TANAKA K., SAKAGUCHI A., KANAI Y., TSURUTA H., SHINOHARA A., TAKAHASHI Y. Heterogeneous distribution of radio cesium in aerosols, soil and particulate matters emitted by the Fukushima Daiichi Nuclear Power Plant accident: retention of micro-scale heterogeneity during the migration of radio cesium from the air into ground and river systems. *Journal of Radioanalytical and Nuclear Chemistry*, **295**, 1927, **2013**.